Available online at www.sciencedirect.com

ScienceDirect

Ceramics International 40 (2014) 4591–4598

CERAMICS INTERNATIONAL

www.elsevier.com/locate/ceramint

Rheological properties and stability of NMP based cathode slurries for lithium ion batteries

Werner Bauer*, Dorit Nötzel

Karlsruhe Institute of Technology, Institute for Applied Materials – Material Process Technology, Hermann-von-Helmholtz-Platz 1, 76344 Eggenstein-Leopoldshafen, Germany

Received 24 June 2013; accepted 31 August 2013
Available online 6 September 2013

Abstract

Slurries for the manufacturing of cathodes for lithium ion batteries are compared regarding to their colloidal stability by means of rheology. Model formulations with nanoscaled $LiFePO_4$ (LFP) and micron scaled $Li(Ni,Mn,Co)O_2$ (NMC) were prepared by using N-methyl-2-pyrrolidone (NMP) as solvent. Polyvinylidene difluoride (PVDF) binder and carbon black (CB) conducting additive were added at typical amounts of a few weight percent. The influence of these inactive electrode components on the physical stability of the dispersions was investigated by steady state and oscillation experiments. It is demonstrated that the addition of a high molecular weight PVDF binder is sufficient to establish gel formation by bridging flocculation in case of the nanoscaled cathode material. For the larger micron scaled particles, the formation of a stable coagulated state is also feasible but it requires the combination of a particulate CB gel and a strengthening PVDF polymer network.
© 2013 Elsevier Ltd and Techna Group S.r.l. All rights reserved.

Keywords: Lithium ion batteries; Electrode manufacturing; Rheology; Viscoelasticity; Yield point

1. Introduction

The theoretical performance of a lithium ion battery is determined by the used electrochemically active and inactive materials. However, this potential will not fully be exploited if the processing of these materials is performed inadequately [1–8]. One of the most critical processing steps in ensuring a cell with high performance and reliability is the manufacturing of the electrodes. In this step, the active materials are deposited on metal foils as porous layers with a typical thickness range of 50–100 μm, for example by doctor blade, comma bar or slot die coating [9]. The coating process must result in layers with very homogenous thickness and density distribution as any inhomogeneity in the layer might result in undesired local aging of the electrode [10].

The most important prerequisite for a controlled coating process is the preparation of homogeneous and stable dispersions of the active materials and supporting inactive components. Basic slurry compositions for cathodes consist of the active material, carbon black (CB) as a conductive agent and polyvinylidene difluoride (PVDF) as a binder. The solvent must have the potential to dissolve PVDF, for which reason N-methyl-2-pyrrolidone (NMP) is used typically. For most cathode materials, like $LiMn_2O_4$ (LMO) or the varieties of $Li(Ni,Mn,Co)O_2$ (NMC), mean particle sizes in the range of 5–10 μm are preferred. Such large particles allow higher solids contents in the electrode layer facilitating a higher energy density. Furthermore, the lower specific surface area of large particles reduces the amount of interaction with the electrolyte – which plays an important role in the degradation of a cell. A different situation exists for lithium iron phosphate $LiFePO_4$ (LFP), which is usually prepared as submicron powder. Submicron sized particles are desirable as the electronic conductivity and the diffusion coefficient of the lithium ions are very low for this material [11]. Even smaller primary particle sizes below 100 nm are typical for CB conductive additives. However, the as-delivered powders contain large agglomerates, which require an efficient de-agglomeration step before or during the mixing of the slurry [12]. Despite this broad range of particle sizes from the nano to the micron scale, it is necessary to prepare a

*Corresponding author. Tel.: +49 721 608 22990; fax: +49 721 608 24612.
E-mail address: werner.bauer@kit.edu (W. Bauer).

0272-8842/$ - see front matter © 2013 Elsevier Ltd and Techna Group S.r.l. All rights reserved.
http://dx.doi.org/10.1016/j.ceramint.2013.08.137

MRD EX. 2020
LGES v MRD
IPR2024-01011

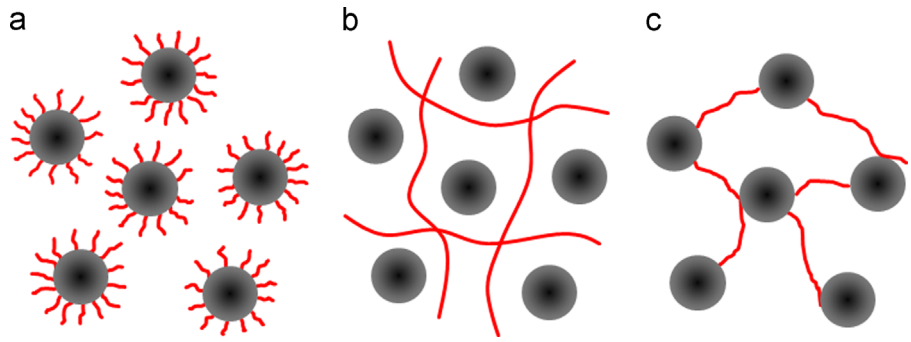

Fig. 1. Particle–polymer-interaction in a dispersion with (a) sterically stabilizing dispersant, (b) thickener and (c) coagulating binder.

homogeneous dispersion for all components. Additionally, it must be stable over a storage time of a few hours as this period can arise from the dwell time of a slurry in storage tanks and feed pipes of the mixing and coating units.

The term stability can be understood in various interpretations. Commonly, stability is defined as the ability of a dispersion to withstand mass or phase segregation, allowing the conservation of a homogeneous particle distribution over a long period of time after the mixing step. Segregation can be caused by sedimentation, coagulation or Ostwald ripening. For colloidal battery slurries, the main problems arise from sedimentation of large active materials or agglomeration of small active and inactive particles.

Resistance to agglomeration or sedimentation may result either from repulsive particle interactions or from attractive forces creating a three dimensional interconnected network. In the first case, a repulsive electrostatic or steric potential energy barrier prevents discrete particles from forming larger agglomerates (Fig. 1a) [13]. However, this condition can suppress sedimentation only for very small particles, where the Brownian motion dominates over gravity allowing these particles to float in the liquid. A lot of active battery materials are in principle too large to be prevented from settling, even if they are stabilized as individual particles.

The term stable is usually relative as it also refers to a state with sufficiently low rate of coagulation or sedimentation. Another way to achieve stability is therefore a reduction of the mobility of the particles in the dispersion. This can be simply realized by increasing the viscosity of a slurry, e.g. by addition of thickening agents (Fig. 1b) [14]. A higher viscosity decreases the kinetic energy of the particles and prevents them from overcoming repulsive energy barriers, and according to Stokes law, reduces the sedimentation speed of the particles. However, the requirements of a coating process involve a castable formulation, therefore limiting the applicable viscosity range. Under these preconditions, an efficient depression of sedimentation effects cannot be achieved by a plain viscosity rise, especially for large particles.

More successful is an approach based on the formation of a weakly coagulated state. In this case, a cohesive, non-touching network is built by individual particles (Fig. 1c), which is voluminous enough to span the container [15,16]. Strong attractive interactions promote flocculation of particles and irreversible destabilization of the dispersion, whereas in a weakly coagulated system the particles form metastable, secondary bond based structures, which hold these particles at distance. Suited systems provide sufficient attraction to stabilize the particle network against gravitational effects like sedimentation of discrete particles. Also, they must have enough load capacity to prevent the particle network from consolidating by its own weight, but can be fluidized even at low shear rates and facilitate reformation on cessation of the flow.

Characteristic for weakly coagulated dispersions is the formation of a gel system with a mild yield point and extensive shear thinning behavior at relatively low solids loading (volume fraction $\Phi \ll 0.6$) [16]. The transformation from an aggregated particle network to a liquid-like system is caused by a gradual disruption of links between the particles. Therefore, it does not take place at a defined shear stress but in a broad transition zone.

In this study, we compare the colloidal stability of various NMP based cathode slurries by means of rheological testing. NMC or LFP active materials and carbon black were used as particulates to cover a broad range of particle sizes from the nano to the micron range. Two commercial PVDF grades, which are specifically recommended for application in lithium ion batteries, were chosen as polymeric binders and compared with emphasis on their influence on the rheology of the pastes.

2. Experimental

Slurries for the manufacturing of cathode coatings were prepared by mixing active cathode materials and CB powder with PVDF resins in NMP without further additives. $LiFePO_4$ (SC/P2, Süd-Chemie AG, Germany) with a median of 130 nm, measured by electroacoustic spectrometry (DT1200, Dispersion Technology, USA) and a BET specific surface of 16 m^2/g (measured by Flowsorb II 2300, Micromeritics, USA) was chosen as an example for a nanoscaled cathode material. The micron size is represented by a $Li(Ni_{1/3}Mn_{1/3}Co_{1/3})O_2$ (NM-3100, Toda America, USA) with a mean particle size of 8.9 μm and a BET surface of 0.4 m^2/g. Densities of the powders were measured by a helium pycnometer (Pycnomatic ATC, Porotec, Germany) with an outcome of 3.46 g/cm^3 for LFP and 4.63 g/cm^3 for NMC.

Emulsion precipitated PVDF binders (KYNAR 761 and KYNAR HSV 900, Arkema Inc., France) were used. Both types represent homopolymers with different molecular weights (KYNAR 761: 370.000–450.000 g/mol, KYNAR HSV 900: 900.000–1.300.000 g/mol). As a conductive additive, carbon black (Super C65, Timcal Ltd., Switzerland) with a BET surface of 62 m^2/g and a mean TEM particle size of 35 nm was used [17].

First of all, the binder was dissolved in NMP (Sigma Aldrich, Germany) at ambient temperature. The mixtures, consisting of powders and binder stock solution, were adjusted with additional NMP to a solid loading of 20 or 30 vol% and a binder content of 5 or 10 wt% (relative to the weight of the dried active material). Carbon black content was adjusted to 4 wt% (also dry weight base of active material). The active material was usually added after dispersing the carbon black. Additionally, a sample of NMC and carbon black were blended in a high speed dry mixer (Hosokawa Micron Nobilta NOB-130, Japan) at 2800 RPM for 10 min before being dispersed in the binder solution. Wet mixing was performed in a vacuum equipped dissolver (VMA Getzmann, Germany) with a maximum speed of 2000 RPM for 30 min.

Sedimentation effects can hardly be detected in the black colored and nontransparent cathode slurries on a short-time level by optical means. Therefore rheological tests are preferred for characterization as these investigations not only provide information about the flowability of a dispersion, but also concern the segregation stability by looking at the response of a resting system under the impact of low forces. Rheological tests were carried out using steady state flow, amplitude and frequency sweep tests. A rheometer (MCR 300, Paar Physica, Austria) with a plate–plate geometry (PP50, gap 1 mm) at a temperature of 25 °C was used for the tests. Measurements were performed immediately after finishing the mixing process, beginning with steady state flow and followed by the oscillation tests. Prior to all measurement runs, the inserted samples were exposed to a two-minute equilibrium period which ensures the correct temperature of the samples and an acceptable level of the residual normal force. Before starting the oscillation tests, the idle time of the residual slurry during the steady state tests was compensated by an additional rotation step within the rheometer (1 min at 50 1/s).

Steady state flow tests were used for the detection of viscosity and shear thinning behavior. For the determination of yield points, strain against shear stress curves were analyzed. However, steady state flow tests provide sufficient information only for purely viscous systems, but an addition of binder changes the rheological behavior to viscoelastic. In this case more detailed information about the dispersion will be obtained by dynamic oscillatory shear measurements [18]. Amplitude sweeps provide information about the product stability, e.g. the strength of the aggregated state. Time dependent response of the dispersion structure to deformations can be obtained by frequency sweeps, ranging from gradual load (low frequency) up to impact (high frequency). This gives an indication of the structure stability for a length of time, e.g. the idle consistence, segregation characteristic, transport stability and longtime storage behavior of dispersions.

A measure of the elastic strength of a dispersion is the cohesive energy E_{coh}, which represents the work required to maintain the spatial particle distribution [19]. E_{coh} can be obtained from the strain γ_{crit} at the end of the linear-viscoelastic region and the magnitude of G′ in the linear-viscoelastic region by the following equation:

$$E_{coh} = \S G' \gamma_{crit}^2$$

It should be noted that there is typically no quantitative correlation between the flow curve yield stress and the dynamic yield stress [20]. However, both can be used for the quantitative evaluation of dispersions as they reflect the response of the physical structure to mechanical impact.

3. Results

Flow curves of freshly prepared slurries with 20 vol% LFP powder and different PVDF binder additives are depicted in Fig. 2. Shear rates in the used doctor-blade coating device are smaller than 100 1/s. Therefore, a shear rate of 50 1/s was defined as a reference value to compare the viscosities of different slurries. For the addition of 5 wt% 761 or HSV binder a viscosity of 1.0 Pa s or 10.8 Pa s was measured, respectively. While the lower viscosity value roughly marks the lower end of the processing range, the higher value stands for the maximum feasible viscosity of the used coating device. With 10 wt% 761 a viscosity of 3.6 Pa s is measured, which is well within the processing window of the used coating device.

All LFP slurries show shear thinning behavior and, more or less, the existence of a yield point. This can be deduced from the extended vertical branch in the low shear rate section of the flow curves. The formation of a yield point becomes more evident in the profile of the strain against shear stress curves with double logarithmic scaling (deformation curves), where it normally appears as an inflection point separating the ranges of elastically deformation and plastic flow. However, due to the viscoelastic nature of the investigated slurries, no sharp kink, but a broad transition zone can be seen in Fig. 3. The start of this transition zone will be usually declared as the yield point. For the LFP slurries, an increasing yield point is resulting at higher viscosity.

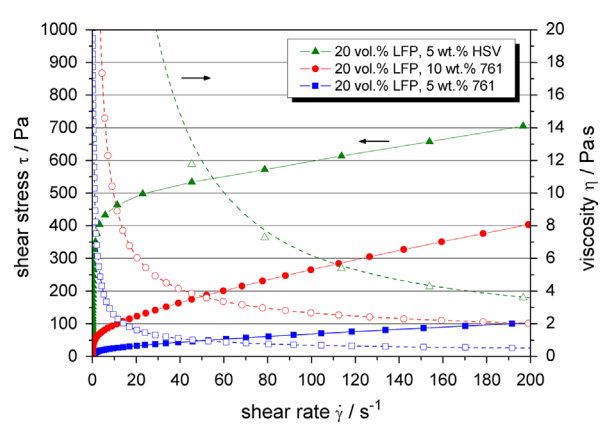

Fig. 2. Flow (filled symbols) and viscosity (unfilled symbols) curves of NMP based slurries with 20 vol% LFP powder and PVDF binders.

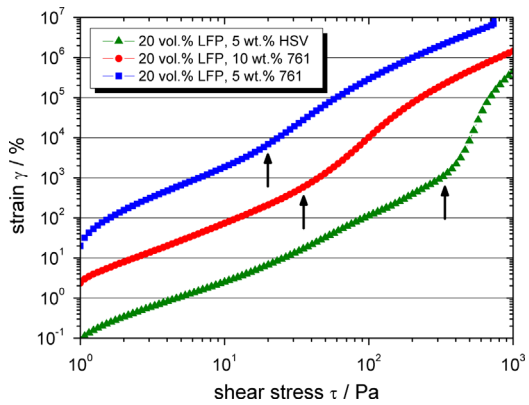

Fig. 3. Deformation curves of NMP based slurries with 20 vol% LFP powder and PVDF binders (arrows refer to yield point of the slurries).

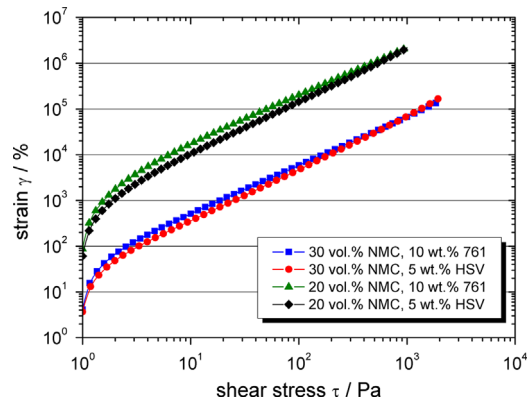

Fig. 5. Deformation curves of NMP based slurries with NMC powder and PVDF binders.

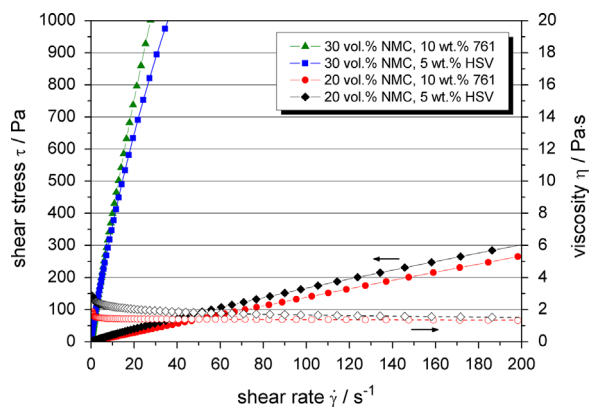

Fig. 4. Flow (filled symbols) and viscosity (unfilled symbols) curves of NMP slurries with NMC powder and PVDF binders.

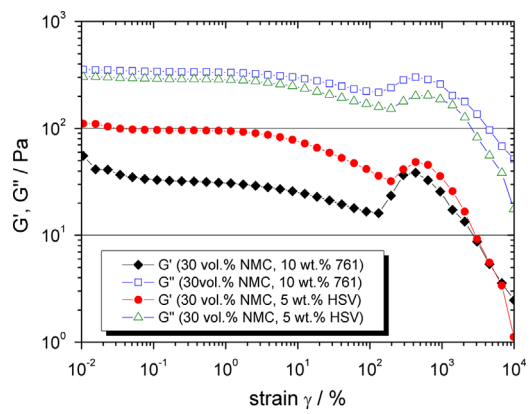

Fig. 6. Amplitude sweeps of NMP based slurries with NMC powder and PVDF binders (angular frequency $\omega = 10\ s^{-1}$).

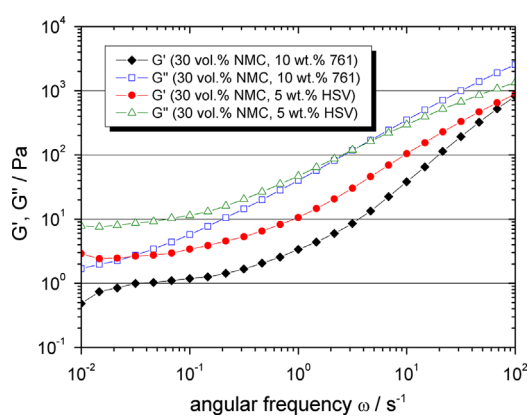

Fig. 7. Frequency sweeps of NMP based slurries with NMC powder and PVDF binders (strain $\gamma = 0{,}1\%$).

Using the coarse NMC powder, the slurries exhibit a much lower viscosity at the same solid content of 20 vol% (Fig. 4) compared to the fine LFP powder. For example, after addition of 5 wt% HSV binder only 1.9 Pa s is received at a shear rate of 50 1/s. The NMC slurries reveal no indication of a yield point and only a slight shear thinning behavior. After increasing the NMC content up to 30 vol%, a distinct viscosity rise takes place, but flow curves (Fig. 4) or deformation curves (Fig. 5) still show no indication of a yield point. This is also affirmed by oscillatory shear measurements. For amplitude sweeps (Fig. 6) as well as for frequency sweeps (Fig. 7), the loss modulus G" dominates over the storage modulus G′. This behavior is typical for fluid type systems which do not reveal a yield point.

The properties of NMC slurries drastically change after an addition of 4 wt% CB. Firstly, the viscosity increases, e.g. from 1.9 Pa s to 6.2 Pa s for the slurry with 20 vol% NMC and 5 wt% HSV (Fig. 8). The CB containing slurries also exhibit shear thinning and a distinct yield point. The existence of a yield point can be recognized in the deformation curves (Fig. 9) and in the oscillatory curves. In case of amplitude sweeps the storage modulus G′ dominates in the low shear range (with a crossover at approximately 10% strain) (Fig. 10) and in frequency sweeps over the whole frequency range (Fig. 11), which is characteristic for a gel type system. The relevance of CB for the formation of the gel structure is also depicted in Fig. 12a and b, at a slurry containing 20 vol% NMC and 4 wt% CB, but no PVDF. Even without the binder, the oscillation measurements show the typical pattern of a gel.

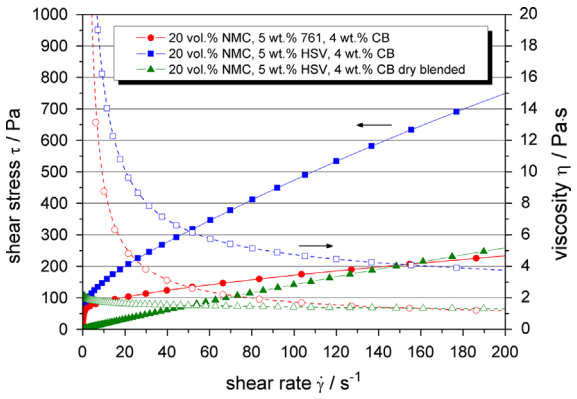

Fig. 8. Flow (filled symbols) and viscosity (unfilled symbols) curves of NMP slurries with NMC powder, PVDF binder and carbon black.

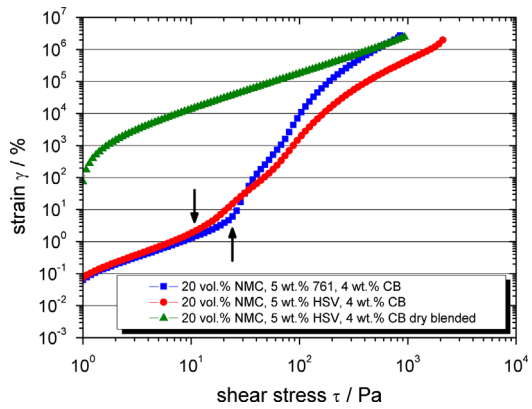

Fig. 9. Deformation curves of NMP slurries with NMC powder, PVDF binders and carbon black (arrows refer to existing yield points of the slurries).

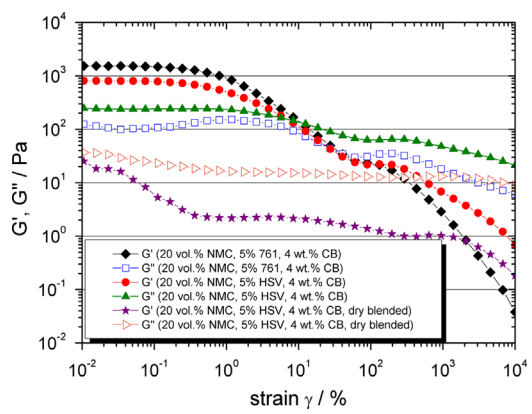

Fig. 10. Amplitude sweeps of NMP based slurries with NMC powder, PVDF binder and carbon black (angular frequency $\omega = 10\ s^{-1}$).

However, if CB is not intermixed to the binder solution as an individual component but dry blended with NMC powder in a high speed mixer at first, gel formation is not observed. In this case the flow behavior is liquid-like and the resulting viscosity is nearly identical to that of the NMC dispersion without CB (Figs. 8–11).

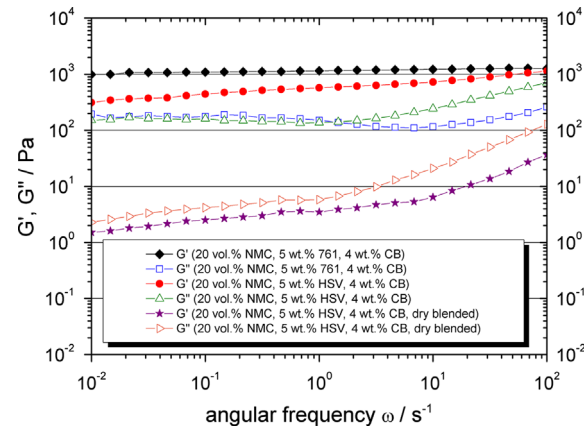

Fig. 11. Amplitude sweeps of NMP based slurries with NMC powder, PVDF binder and carbon black (strain $\gamma = 0{,}1\%$).

4. Discussion

Comparing slurries with identical volume content of solids and identical binder mass fraction but without CB reveals that the dispersions with LFP powder form a gel type structure while NMC dispersions are exhibiting a fluid type behavior. It has to be taken into account that the absolute binder content for the NMC slurry is higher due to the higher density of this active material. Nevertheless, this difference persists even at high viscosities. The reason seems to be the distinct difference in the particle size of the active materials which is nearly seventy times larger for the NMC. A variation in the chemical nature of the particle surface might also be an explanation. However, this seems not to be the case, as further experiments with a larger, micron sized LFP (not presented here) also exhibit a fluid type behavior.

The hypothetical contour length of an unbranched PVDF macro molecule in stretched configuration can be estimated from the size of the orthorhombic unit cell in the *c*-direction (0.462 nm [21]). For a homopolymer PVDF ($-CH_2CF_2-$) with a molecular weight of 400.000 g/mol an approximate chain length of 2.9 µm and 7.2 µm for 1.000.000 g/mol can be calculated, respectively. However, in solution the polymer chains should not exist in stretched configuration but form a random coil structure whose dimensions also depend on its interaction with the solvent. As NMP is a good solvent for PVDF the macromolecules will expand in this solvent. Lutringer and Weill determined the *z*-average radius of gyration of various PVDF samples in NMP by light-scattering experiments [22]. Exemplary results were 44.1 ± 5.0 nm and 74.2 ± 6.0 nm for molecular weights of $(310 \pm 10) \times 10^{-3}$ g/mol and $(702 \pm 20) \times 10^{-3}$ g/mol respectively. The radius of gyration is defined as the quadratic mean distance of the collection of monomers from their common center of gravity. It is smaller than the hydrodynamic radius but allows an estimation of the molecular size as the majority of the monomers is located within a spherical shell with the radius of gyration. From these results it can be derived that in solution the characteristic diameters of the used PVDF molecules are set in the range of 100–200 nm, i.e. roughly at

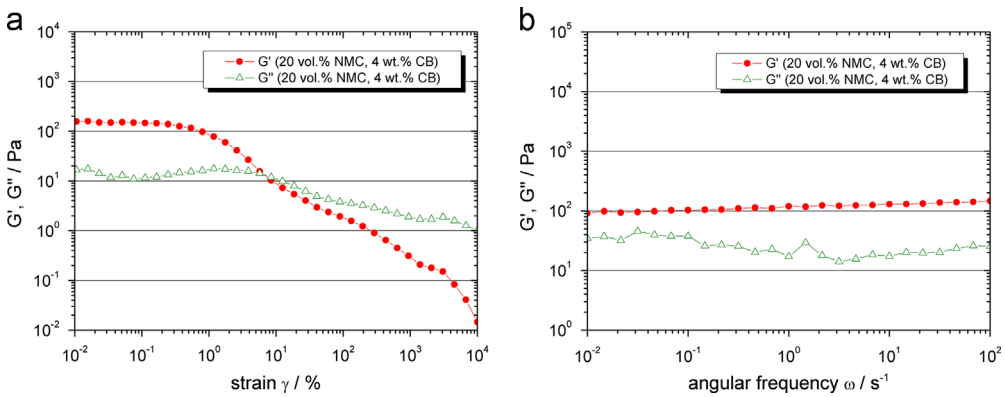

Fig. 12. Amplitude (a) and frequency (b) sweeps of NMP based slurries with NMC powder and carbon black, but without binder.

the size of the LFP powder, but larger than the carbon black particles and significantly smaller than the NMC particles.

A change in the configuration of the PVDF occurs when the molecule gets into contact with a solid interface. Parts of the polymer chain can adsorb at the surface of the particles forming so-called trains, while other parts extend into the solvent as loops or tails [24]. This process is fairly complicated as it involves polymer/surface interaction, polymer/solvent interaction and the configuration of the polymer chain. However, it can be expected that at low adsorption energy extended loops or tails are favored, whereas at high adsorption energy, long trains and short loops or tails predominate, leading to a more flattened conformation.

An absorbed PVDF polymer layer prevents direct contact of particle surfaces and has therefore the potential to stabilize a suspension against agglomeration. However, extended polymers can also interact with other particles or another adsorbed polymer layers. Especially, when segments of one polymer chain adsorb on different particles aggregation takes place by bridging flocculation. On large particles with a high number of interacting sites a more flat configuration of the binder molecule is probable. This arrangement decreases the probability of interaction with other particles. Small particles, on the other hand, provide less adsorption sites for a single binder molecule. In this case, the polymer chains tend to protrude from the surface. If this leads to the entanglement of polymer chains or bridging of two or more particles, a gelled network is formed.

If the binder molecules are considerably smaller than the particles, also a significant portion of the binder can deposit at locations where the distance to the next particle gets so large that bridging becomes unlikely. In that case the molecules become inactive as they do not play a role for the formation of an attractive network.

It is known from PVDF/$LiCoO_2$ composites that they exhibit only poor binder/particle interfacial adhesion [23]. Due to the related chemical surface, this should also be valid for NMC. In combination with the reduced number of bonds due to the lower number of particles, the overall attractive interaction in the NMC particle network is reduced in such a way that structural breakdown is induced even at low shear stresses, not allowing the formation of a stable gel.

Table 1
Cohesive energy E_{coh} of slurries with 20 vol% NMC+4 wt% carbon black.

Binder	$E_{coh}/10^{-6}$ J/m^3
No binder	198
5 mass% 761	1975
5 mass% HSV	1045

These arguments provide explanations for the improved stability of submicron LFP particles in contrast to the much larger NMC particles in a pure binder solution. However, slurries containing micron sized NMC particles also have the capability to form a coagulated structure by the addition of nanoscaled CB particles. CB can be electrostatically stabilized in NMP without additional dispersants as these particles are charged by counterions from dissociating surface groups [25]. For NMC, on the other hand, the attractive van-der-Waals forces seem to dominate as dispersions without stabilizing agents were found to show intense flocculation tendency. It is known that dispersions with mixtures of attractive microparticles and repulsive nanoparticles with a high size ratio form a colloidal gel at high and low nanoparticle content, respectively, while at intermediate nanoparticle volume fractions a stable colloidal fluid can exist [26]. Gel formation can also be observed in the oscillation measurement results for NMC/CB mixtures. However, without binder these gels are not very robust; they do not support their own weight and settle quickly. For adequate gel strength, the addition of polymer binders is required. The influence of a binder on the elastic strength of a gel is also depicted by a large increase of the cohesive energy E_{coh} (Table 1). It is noticeable that the high molecular weight binder (HSV) produces a lower gel strength produces a lower corresponding yield point (Fig. 9), despite an increased slurry viscosity. An explanation might be a time dependent buildup of the cohesive network which is retarded for binders with extended molecular chains.

One reason for the stabilizing effect of the binders used here might be the affinity of CB nanoparticles to PVDF. In SEM micrographs of dried electrodes it can be typically observed that CB is not homogeneously distributed on the surface of the cathode material (Fig. 13). Rather, binder and CB form a film which provides an interconnecting conductive network and

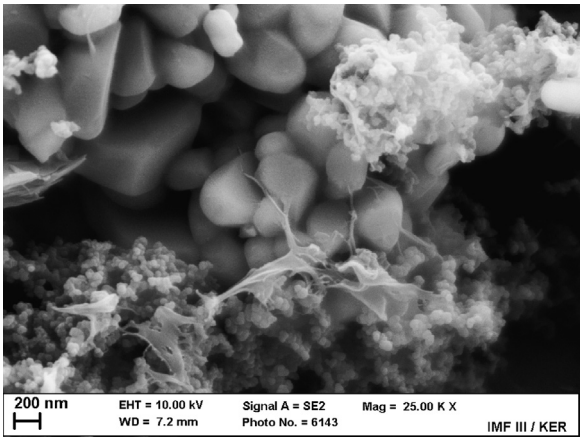

Fig. 13. SEM micrograph of a NMC cathode particles with adhering PVDF/carbon black clusters.

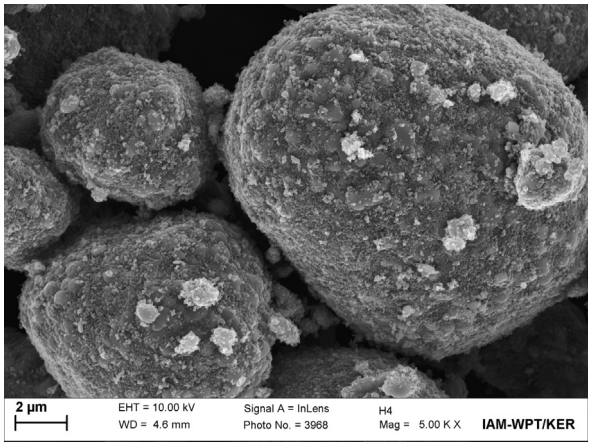

Fig. 14. SEM micrograph of NMC particles after dry blending with carbon black. NMC particles are covered with the fixed carbon black particles.

simultaneously links the NMC particles together. This is also consistent with the results of Zheng et al. [27], where the PDVF consuming effect of carbon nanoparticles was depicted. It is probable that this type of interaction already exists in the suspension state. The consequence would be that a homogeneous distribution of CB is disrupted in the slurry by the PVDF binder as a fraction of the nanoparticles is already trapped in the polymer matrix. Gel formation would then mainly be supported by the interaction of the nanoparticles with the entangled polymer chains.

The influence of carbon black nanoparticles on the stability of NMC slurries becomes similarly visible by premixing the particulate components in a high-speed dry mixer. By this process, the carbon black particles are firmly bound as deposits on the surface of the NMC particles (Fig. 14), where they even withstand the subsequent slurry mixing step. This immobilization has severe consequences on the rheology as the resulting slurries become incapable of building a percolation structure. The flow behavior is nearly identical to slurries without CB, i.e. no yield point exists and the NMC particles are not stabilized against segregation.

5. Conclusion

Binder and carbon black are essential components of electrodes for lithium ion batteries. The main function of the binder is the improvement of the mechanical strength and the adhesion of the electrode on the current collector. Carbon black is added to increase the electrical conductivity of the electrode. However, both additives also play an important role during slurry preparation and electrode processing. One vital aspect is the stabilization of slurries against segregation, mostly against sedimentation of the particles. Instead of stabilizing the colloids against any form of aggregation, it is more beneficial to promote weak coagulation of these dispersions. Weak attractive forces can stabilize homogeneous particle systems by the development of a gel network, which immobilizes the particles. However, the strength of attraction must be adjusted properly in order to withstand gravity, but also to prevent the formation of a robust network which does not allow complete fluidization for the electrode coating process.

In the case of the nanoscaled LFP powder, the addition of a PVDF binder with sufficient long chain length was found to cause gel formation in NMP by bridging flocculation. The micron sized NMC particles in association with the comparably small binder molecules did not allow a creation of a stable polymer gel structure. Here, the addition of nanosized carbon black was necessary to provide attraction between the NMC particles by formation of a particulate gel. However, the PVDF binder also became important, as only the combination of polymer and particulate additives provided sufficient gel strength to stabilize the large NMC particles against rapid sedimentation.

It should be noted, that additives, like binder or carbon black, are chosen and optimized predominantly for their impact on the electrochemical properties of the electrode. It is a fortunate coincidence, that frequently used battery compositions also have a beneficial influence on the colloidal stability of the slurries. The supplementary relevance of these components for slurry processing is thus often overlooked. However, since a stabilizing effect cannot be expected for all compositions, it is of advantage to know more about these relationships.

References

[1] R. Dominko, M. Gaberscek, J. Drofenik, M. Bele, S. Pejovnik, J. Jamnik, The role of carbon black distribution in cathodes for Li ion batteries, Journal of Power Sources 119–121 (2003) 770–773.

[2] S. Kuroda, N. Tobori, M. Sakuraba, Y. Sato, Charge–discharge properties of a cathode prepared with ketjen black as the electro-conductive additive in lithium ion batteries, Journal of Power Sources 119–121 (2003) 924–928.

[3] E. Ligneel, B. Lestriez, D. Guyomard, Relationships between processing, morphology and discharge capacity of the composite electrode, Journal of Power Sources 174 (2007) 716–719.

[4] E. Ligneel, B. Lestriez, A. Hudhomme, D. Guyomard, Shaping of advanced ceramics: the case of composite electrodes for lithium batteries, Journal of the European Ceramic Society 29 (2009) 925–929.

[5] T.J. Patey, A. Hintennach, F. La Mantia, P. Novák, Electrode engineering of nanoparticles for lithium-ion batteries—role of dispersion technique, Journal of Power Sources 189 (2009) 590–593.
[6] G.-W. Lee, J.H. Ryu, W. Han, K.H. Ahn, S.M. Oh, Effect of slurry preparation process on electrochemical performances of $LiCoO_2$ composite electrode, Journal of Power Sources 195 (2010) 6049–6054.
[7] G. Mulder, N. Omar, S. Pauwels, M. Meeuse, F. Leemans, B. Verbrugge, W. de Nijsd, P. van den Bossche, D. Six, J. van Mierlo, Comparison of commercial battery cells in relation to material properties, Electrochimica Acta 87 (2013) 473–488.
[8] H.Y. Tran, G. Grecoa, C. Täubert, M. Wohlfahrt-Mehrens, W. Haselrieder, A. Kwade, Influence of electrode preparation on the electrochemical performance of $LiNi_{0.8}Co_{0.15}Al_{0.05}O_2$ composite electrodes for lithium-ion batteries, Journal of Power Sources 210 (2012) 276–285.
[9] R.J. Brodd, K. Tagawa, Lithium-ion cell production processes, in: W. A. van Schalkwijk, B. Scrosati (Eds.), Advances in Lithium-Ion Batteries, Kluwer Academic/Plenum Publishers, New York, 2002.
[10] T. Takamura, M. Saito, A. Shimokawa, C. Nakahara, K. Sekine, S. Maeno, N. Kibayashi, Charge/discharge efficiency improvement by the incorporation of conductive carbons in the carbon anode of Li-ion batteries, Journal of Power Sources 90 (2000) 45–51.
[11] P.P. Prosini, M. Lisi, D. Zane, M. Pasquali, Determination of the chemical diffusion coefficient of lithium in $LiFePO_4$, Solid State Ionics 148 (2002) 45–51.
[12] C.-C. Chang, L.-J. Her, H.-K. Su, S.-H. Hsu, Y.T. Yen, Effects of dispersant on the conductive carbon for $lifepo_4$ cathode, Journal of the Electrochemical Society 158 (2011) A481–A486.
[13] S. Zürcher, T. Graule, Influence of dispersant structure on the rheological properties of highly-concentrated zirconia dispersions, Journal of the European Ceramic Society 25 (2005) 863–873.
[14] T.F. Tadros, Applied Surfactants: Principles and Applications, Wiley-VCH Verlag GmbH & Co. KGaA, Weinheim, 2005.
[15] J. Davies, J.G.P. Binner, Coagulation of electrosterically dispersed concentrated alumina suspensions for paste production, Journal of the European Ceramic Society 20 (2000) 1555–1567.
[16] J.A. Lewis, Colloidal processing of ceramics, Journal of the American Ceramic Society 83 (2000) 2341–2359.
[17] M.E. Spahr, E. Grivei, D. Goers, New carbon conductive additives for advanced lithium ion batteries, in: Proceedings of LLIBTA Europe, Mainz, Germany, February 3, 2010.
[18] T.G. Mezger, The Rheology Handbook, second ed., Vincentz Network, Hannover, 2006.
[19] D. Megías-Alguacil, Characterization of the linear viscoelastic region in suspensions of zirconium oxide: cohesive energy obtained from the critical parameters, Applied Rheology 14 (2004) 126–132.
[20] I. Masalova, A.Y. Malkin, R. Foudazi, Yield stress of emulsions and suspensions as measured in steady shearing and in oscillations, Applied Rheology 18 (2008) 44790-1–44790-8.
[21] B. Ameduri, From vinylidene fluoride (VDF) to the applications of vdf-containing polymers and copolymers: recent developments and future trends, Chemical Reviews 109 (2009) 6632–6686.
[22] G. Lutringer, G. Weill, Solution properties of poly(vinylidene fluoride): 1. Macromolecular characterization of soluble samples, Polymer 32 (1991) 877–883.
[23] S. Babinec, H. Tang, A. Talik, S. Hughes, G. Meyers, Composite cathode structure/property relationships, Journal of Power Sources 174 (2007) 508–514.
[24] G.J. Fleer, M.A. Cohen Stuart, J.M.H.M. Scheutjens, T. Cosgrove, B. Vincent, Polymers at Interfaces, Chapman and Hall, London, 1993.
[25] A. Basch, R. Horn, J.O. Besenhard, Substrate induced coagulation (SIC) of nano-disperse carbon black in non-aqueous media: the dispersibility and stability of carbon black in N-methyl-2-pyrrolidinone, Colloids and Surfaces A: Physicochemical and Engineering Aspects 253 (2005) 155–161.
[26] V. Tohver, A. Chan, O. Sakurada, J.A. Lewis, Nanoparticle engineering of complex fluid behavior, Langmuir 17 (2001) 8414–8421.
[27] H. Zheng, R. Yang, G. Liu, X. Song, V.S. Battaglia, Cooperation between active material, polymeric binder and conductive carbon additive in lithium ion battery cathode, Journal of Physical Chemistry C 116 (2012) 4875–4882.